

Preparation and characterization of SiO₂-enhanced TiO₂ thin films for solar cell applications

M. Q. Fahem^a, H. N. Mohsion^a, Z. T. Turki^b, H. A. R. Abdullah^c,
M. H. Jawad^{a*}

^a Department of Medical Physics, College of Applied Medical Sciences, University of Kerbala, Karbala, Iraq

^b College of Health and Medical Technologies/ Department of Anesthesiology University of Al Zahraa for Women/Karbala/Iraq

^c Department of Environmental Health, College of Applied Medical Sciences, University of Karbala, Karbala, Iraq

Titanium oxide has excellent optical and chemical properties, which makes it an important and good element in many applications. Adding other elements to titanium will improve many of its properties, especially SiO₂. This research deals with how these effects can improve the general properties of titanium by adding different ratios of SiO₂ and how these ratios affect the crystal structure and optical and chemical properties of the prepared films. The sol-gel method was used and a broad analytical view of the effect of silica on the surface shape and energy gap of thin films was presented. In this research, we adopted the ratios between SiO₂:TiO₂ (1:0.1, 1:0.2, 1:0.3 and 1:0.4). The tests that were conducted were represented by X-ray diffraction, infrared spectrum, scanning electron microscope (SEM), and atomic force microscope (AFM). To be applied in the solar cell system, the results showed a significant improvement in the performance of the solar cell at certain doping ratios compared to other ratios. Results reveal that SiO₂ doping promotes an amorphous phase in TiO₂, alters surface morphology, and impacts optical properties, making the composite material suitable for applications in photocatalysis and environmental remediation. In addition, the performance of these films in solar cell applications was evaluated, with results showing a significant improvement in power conversion efficiency, opening a new horizon for their use in upgrading the execution of solar cells.

(Received April 10, 2025; Accepted July 11, 2025)

Keywords: Sol-gel method, SiO₂, TiO₂, AFM, SEM, XRD, Solar cells

1. Introduction

With the ever-increasing global energy demands and the limitation of readily available conventional fuels, the pursuit of alternative energy sources, especially solar energy, has become of paramount importance [1]. Despite the obvious benefits of adopting solar cells, they must be economical and affordable with standard energy sources, as all scientific or breakthrough developments must be balanced against the associated cost [2]. Solar cells demonstrate an efficient and ready-to-implement technology for future energy installations. They provide equivalent power conversion efficiency (PCE) with low material and manufacturing costs. Titanium dioxide (TiO₂) is inexpensive, abundant, and environmentally friendly [3]. TiO₂ has been widely used in photo-assisted response, water filtration for hydrogen production in solar photovoltaic cells, and more [4, 6]. Amidst this application, remarkably, TiO₂ has been applied as a great solar catalyst for removing harmful natural pollutants [7,8]. However, the unnecessary use of light in VL or sunlight and the low quantum energy efficiency of photocatalytic responses, which are respectively due to the relatively wide band gap of 3.0–3.2 Å that requires UV exposure to stimulate them [9] and the high rate of electron-hole (e-h) dimer reconstruction, restrict their applications to the spectacular range

* Corresponding authors: mohammed.hamza@uokerbala.edu.iq
<https://doi.org/10.15251/JOR.2025.214.419>

[10]. The large band gap in the photonic range requires that the small-sized TiO_2 fragments are isolated and recovered much more strongly than in the modified mixture [11]. Thus, the efficient partitioning of electron-hole (e-h) conformations and the extension of the gap lifetime are very beneficial for the photodegradation reaction. Anatase, rutile, and brookite are all possible crystalline phases of TiO_2 , each with a distinct chemical and structural structure. [12,13]. The most stable form of TiO_2 is rutile. Sol-gel is one of the most successful methods for fabricating high-nanometer (photocatalytic TiO_2) structures [14]. Due to the high purity and high homogeneity, in addition to the lack or little need for temperature control, this technology is excellent for application. [15].

TiO_2 is a semiconductor element with good conductivity and is widely used in many applications that include improving optical and electrical properties. [16-18] Despite the wide use of these elements, there are some limitations or restrictions that may affect the results, including that the energy gap is considered relatively large (about 3.0-3.2 eV) in addition to the low consumption of the visible spectrum. In order to confront and overcome these limitations, many methods have been proposed, one of which is doping titanium dioxide with silica, which is considered an effective technology in this regard [19].

In addition to the fact that titanium has been widely studied, silica has also been widely studied due to its many properties and advantages and its high ability to influence the crystalline, surface and electrical properties of titanium, as it effectively helps to increase the rate of light scattering as well as reduce the effect of the electron gap, which causes energy loss and dissipation. All of these reasons have made silica an effective element in solar cell applications [20].

In recent years, researchers have focused on the phenomenon of solar cells and their development due to the low costs provided by this technology, as well as the reduction in fuel consumption rate, in addition to the fact that it is considered environmentally friendly and does not cause pollutants [21]. By using titanium dioxide as a basic component in our research, we were able to obtain good energy conversion efficiency. Solar cell technology has provided good efficiency at low costs in a way that is considered safe and environmentally friendly, which enhances its role in providing energy needs that will be increasingly in demand, especially in the future [22].

2. Experimental part

2.1. Materials and methods

Titanium dioxide and silica with purity of 99.0% were purchased from Tecnan, Spain. Titanium isoprenoid $\text{Ti}[\text{OCH}(\text{CH}_3)]$ and tetraethyl orthosilicate ($\text{Si}(\text{OC}_2\text{H}_5)_4$) were used as raw materials for titanium dioxide and silica, and the dissolution of these elements using ethanol and acetic acid was purchased from SCM-Aldrich.

2.2. Synthesis of $\text{TiO}_2\text{:SiO}_2$ thin films

Ethanol and acetic acid were used as solvents to prepare TiO_2 and SiO_2 solutions. The TiO_2 solution was prepared by mixing isoprene titanate with ethanol and acetic acid under continuous stirring. The SiO_2 solution was prepared by hydrogenating tetraethyl orthosilicate using ethanol and water. After preparing these solutions, they were combined in different ratios (1:0.1, 1:0.2, 1:0.3, and 1:0.4), and the resulting gel was deposited on glass slides by spin-coating. The resulting films were then dried at 80°C , followed by an annealing for 10 hours at 450°C to ensure film stability. Figures 1 illustrate the preparation of the gel and thin films.

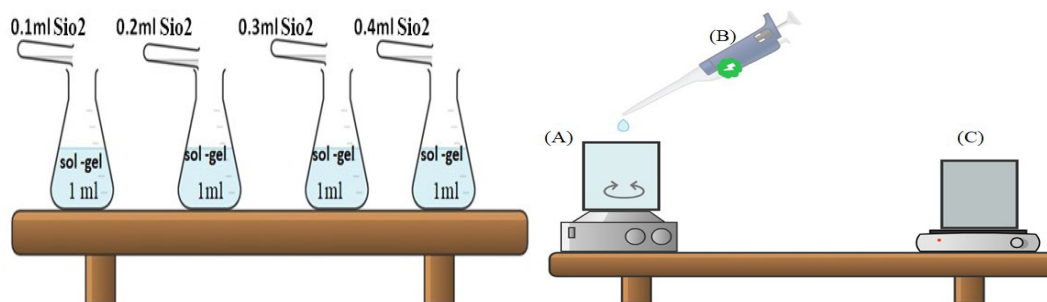


Fig. 1. The different ratio dopant of TiO_2 sol-gel: SiO_2 and preparation thin films.

2.3 Characterization techniques

Using X-ray diffraction (XRD), analyze the phase composition, crystallite size, and crystal structure of the films, providing insight into their structural properties. Fourier transform infrared spectroscopy (FTIR) was conducted to recognize operational sets, confirm the incorporation of SiO_2 , and detect any possible chemical interactions. SEM, or scanning electron microscopy, was used to investigate the surface shape and size of the particles, and the uniformity of the films, while atomic force microscopy (AFM) provided detailed measurements of surface roughness, film uniformity, and topographical features. To ascertain the optical band gap, assess the light absorption characteristics, and investigate the films' potential for optical and electrical applications, the optical investigation was also carried out using UV-Vis spectroscopy.

3. Results and discussion

3.1. Structural analysis

Figure 3 displays the XRD patterns of the TiO_2 thin films doped with SiO_2 at various ratios (1:0.1, 1:0.2, 1:0.3, and 1:0.4). Pure TiO_2 showed a combination of rutile and anatase phases, according to XRD examination. In the sample containing only TiO_2 , the anatase phase clearly appears at angles 25.29° (peak at (101)) and 47.90° (peak at (200)), while the rutile phase appears at angle 27.48° (peak at (110)). When SiO_2 was added to TiO_2 , a gradual shift toward the amorphous phase was observed with increasing SiO_2 ratio. In the sample with a 0.1 SiO_2 ratio, anatase remained the dominant phase, but as the ratio increased to 0.2, some changes in the intensity of the crystalline peaks began to appear, especially at 25.29° , indicating the influence of SiO_2 in disrupting the crystal growth. As the SiO_2 ratio increased to 0.3 and 0.4, the transformation to the amorphous phase became more obvious, and the intensity of the crystalline peaks of titanium decreased significantly. This change reflects the effect of SiO_2 in reducing the crystal order and transforming the crystal structure towards the amorphous phase [8].

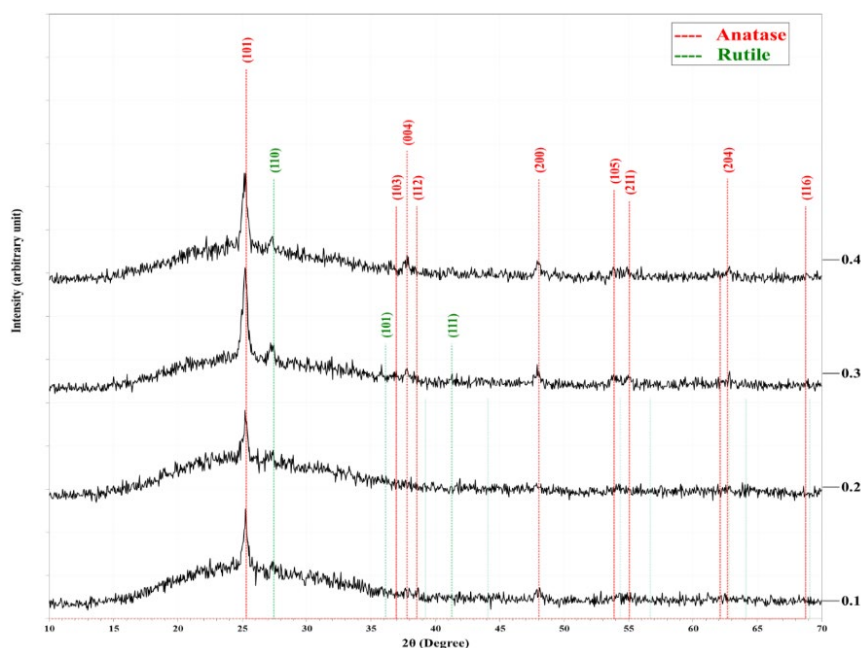


Fig. 3. XRD patterns of $\text{TiO}_2\text{:SiO}_2$ thin films with different SiO_2 doping ratios.

In the samples containing only TiO_2 , the anatase phase is clearly visible at angles of 25.29° and 47.90° , while the rutile phase is visible at angle 27.48° . As the SiO_2 ratio increases, its effect begins to modify the crystal structure, with changes in the strength from a crystalline summit observed. During the sample with a SiO_2 ratio of 0.1, the anatase phase remains dominant, but as the SiO_2 ratio increases to 0.2 and 0.3, the peaks gradually disappear, indicating a transformation towards the amorphous phase. In the sample with a SiO_2 ratio of 0.4, the crystalline peaks become less clear, demonstrating the effect of SiO_2 in disrupting the crystalline structure of TiO_2 and gradually transforming it into an amorphous phase. Table 1 shows the XRD parameters for TiO_2 doped with SiO_2 at different weight ratios.

Table 1. X-ray diffraction parameters for TiO_2 doped with SiO_2 at different weight ratios.

x	2θ (Deg.)	FWHM (Deg.)	DHL Exp.(Å)	C.S (nm)	hl	Phase
0.1	25.29	0.5080	3.5185	16.0	(101)	Anatase TiO_2
	27.48	0.6604	3.2435	12.4	(110)	Rutile TiO_2
	47.90	0.7620	1.8976	11.4	(200)	Anatase TiO_2
0.2	25.24	0.4572	3.5255	17.8	(101)	Anatase TiO_2
	27.32	0.6604	3.2613	12.4	(110)	Rutile TiO_2
0.3	25.24	0.5080	3.5255	16.0	(101)	Anatase TiO_2
	27.43	0.5080	3.2494	16.1	(110)	Rutile TiO_2
	35.81	0.4572	2.5055	18.2	(101)	Rutile TiO_2
	47.90	0.4064	1.8976	21.4	(200)	Anatase TiO_2
0.4	25.19	0.4572	3.5325	17.8	(101)	Anatase TiO_2
	27.32	0.3556	3.2613	23.0	(110)	Rutile TiO_2
	37.84	0.4572	2.3756	18.4	(004)	Anatase TiO_2
	47.95	0.5080	1.8957	17.1	(200)	Anatase TiO_2

3.2 Morphological analysis

The surface morphology of the $\text{TiO}_2\text{:SiO}_2$ thin films was analyzed using SEM and AFM. SEM images (Figure 4) revealed that the TiO_2 particles were uniformly distributed on the substrate, with particle sizes decreasing as the SiO_2 doping ratio increased. For the $\text{TiO}_2\text{:SiO}_2$ (1:0.1) sample,

the particles were approximately 30 nm in size, while for the $\text{TiO}_2\text{:SiO}_2$ (1:0.4) sample, the particle size was reduced to around 20 nm.

- $\text{TiO}_2\text{:SiO}_2$ (1:0.1): Particle size ~30 nm
- $\text{TiO}_2\text{:SiO}_2$ (1:0.4): Particle size ~20 nm

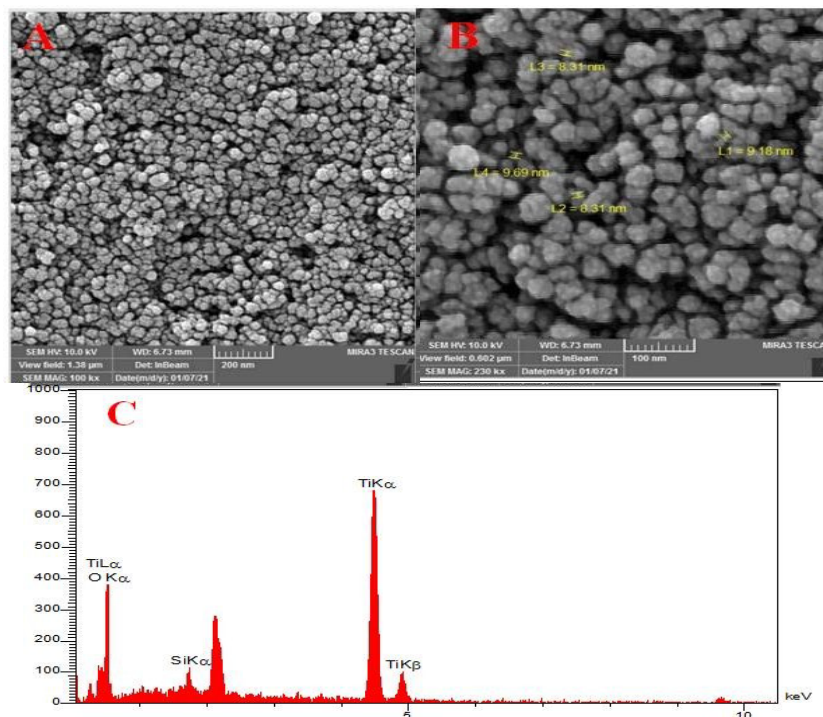


Fig. 4. Nanoparticles of $\text{TiO}_2\text{:SiO}_2$ (1:0.1) prepared without Dye A: SEM B: Effective Zone Pointer Dimensions and C: Energy Dispersive Spectrum.

Figure 5 shows a 3- topological picture of the film surface in three dimensions the image we can conclude that the SiO_2 -coated TiO_2 spherical particles have a diameter of the order of nm. The surface morphology of the TiO_2 thin films changes with the different ratios of SiO_2 . The Nano grain size accumulation distribution for different ratios of SiO_2 without dye shows appearing the increase of SiO_2 leads to increasing in the roughness values. Table 2, has details of the morphology parameter. This result can be attributed to the nucleation process which is associated with the presence of TiO_2 particles taking into belief the clear effect of this inclusion in the nucleation and growth. The rates of heights in the samples ranged from 28.9 to 49.39 nm, while the smallest parameter we obtained was at the grain diameter ratio of 45.97nm.

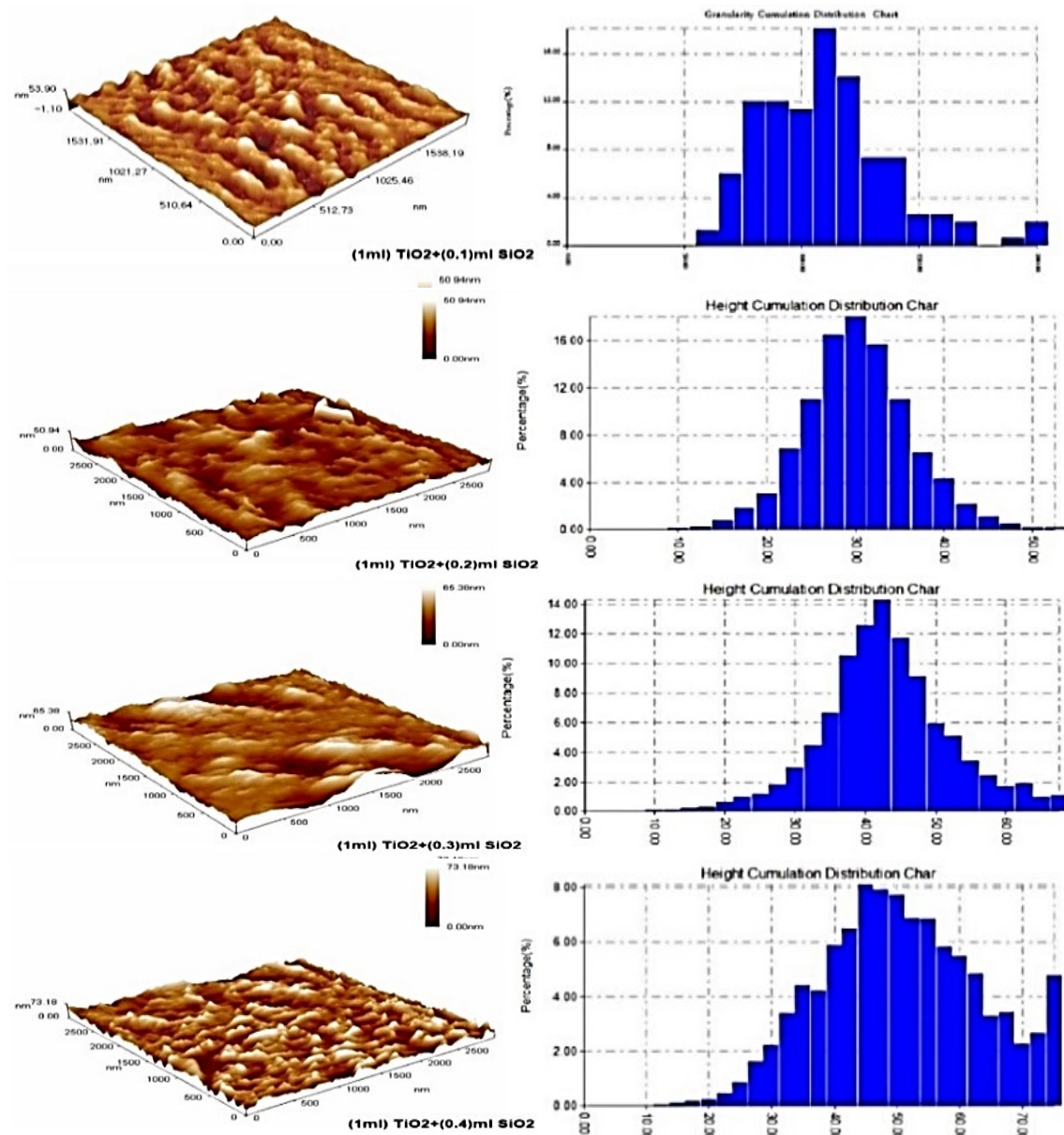


Fig. 5. AFM images of $\text{TiO}_2:\text{SiO}_2$ thin films with different doping ratios showing surface roughness.

Table 2. Morphology parameters of $\text{TiO}_2:\text{SiO}_2$.

$\text{TiO}_2:\text{SiO}_2$ ml	Avg. Height NM	Avg. Diameter nm	Roughness average nm	Root mean square nm
1:0.1	28.9	105.87	5.81	7.52
1:0.2	29.02	54.35	5.04	6.67
1:0.3	41.71	45.97	7.07	9.52
1:0.4	49.39	60.82	10.2	12.8

The increase in roughness values with higher SiO_2 concentrations indicates the presence of more pronounced surface features, which may enhance the photocatalytic activity of the films by increasing the surface area available for reactions. In addition, the variation in grain size distribution and topological dimensions may affect the optical properties of TiO_2 films, impacting their

efficiency in applications such as solar cells and sensors. These morphological features, facilitated by SiO₂ modification, suggest a modifiable approach to improve the functional properties of TiO₂ films based on the requirements of the intended applications. Future studies could explore the direct relationship between the morphological features of these composite films and their functional performance[1].

3.3. Optical properties

UV-Vis spectroscopy was used to study the optical properties of TiO₂:SiO₂ thin films. The absorption spectra (Figure 6) showed that SiO₂ doping slightly increased the optical band gap of TiO₂ from 3.2 eV (for pure TiO₂) to 3.4 eV for the TiO₂:SiO₂ (1:0.4) sample. This shift is due to the increased amorphous content and quantum confinement effects in the nanostructures.

- Pure TiO₂: Band gap ~3.2 eV
- TiO₂:SiO₂ (1:0.4): Band gap ~3.4 eV

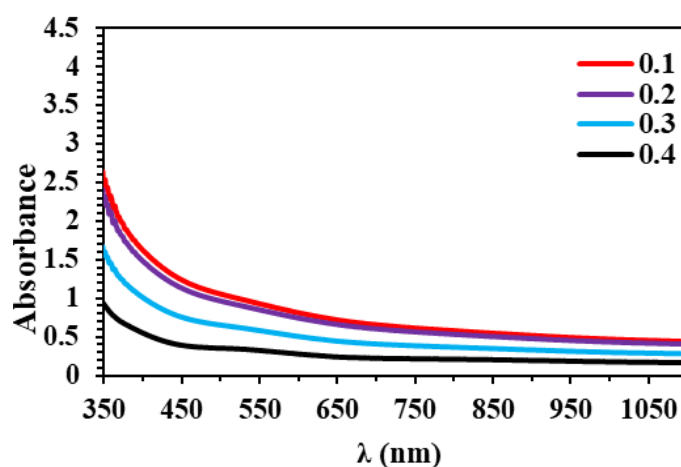


Fig. 6. UV-Vis absorption spectra of TiO₂:SiO₂ thin films with different doping ratios.

The widening of the band gap could be beneficial for applications where higher energy absorption is required, such as in photocatalytic degradation or solar cell applications [23].

FTIR spectra (Figure 7) confirmed the incorporation of SiO₂ into the TiO₂ matrix by showing a distinct Si-O-Ti bond stretching vibration at approximately 1080 cm⁻¹. This was observed for all SiO₂-doped samples, with increasing intensity as the SiO₂ doping ratio increased, indicating a higher degree of bonding between TiO₂ and SiO₂.

- Characteristic Si-O-Ti bond observed at ~1080 cm⁻¹
- Increase in intensity with higher SiO₂ doping ratios

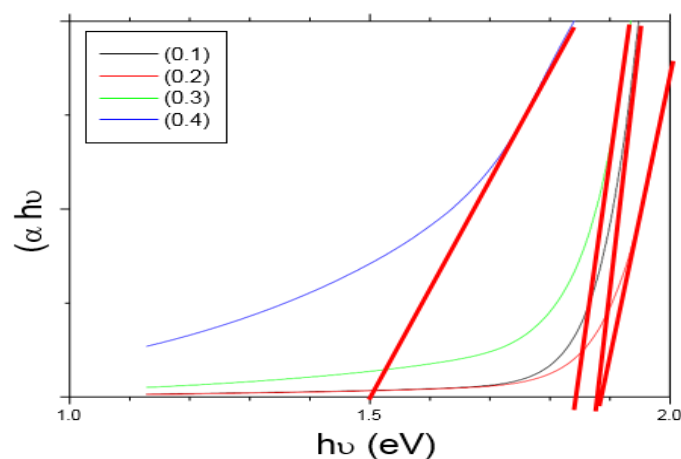


Fig. 7. Tauc relation for TiO_2 doped with SiO_2 at different weight ratios.

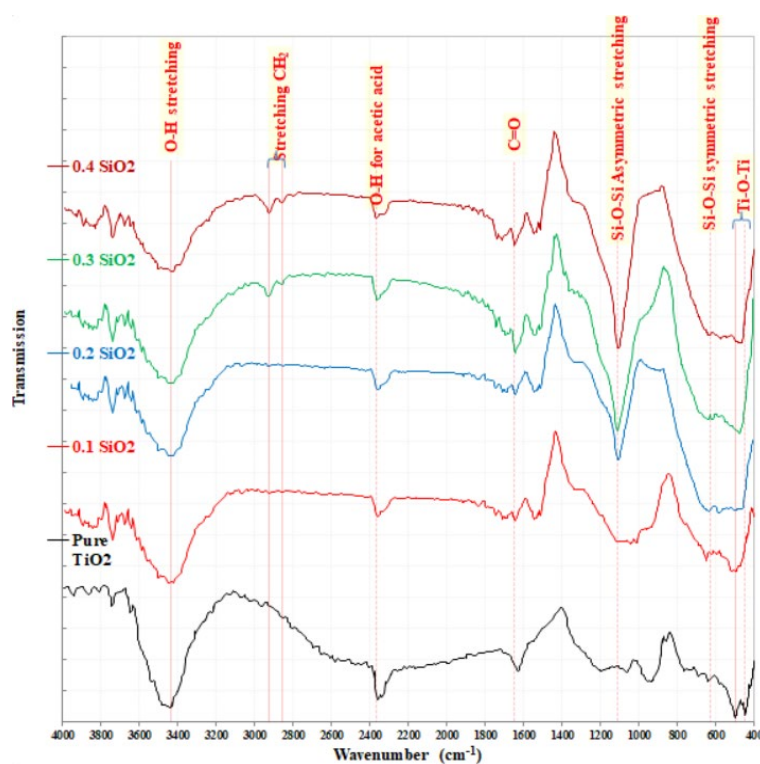


Fig. 8. FTIR spectra of $\text{TiO}_2\text{:SiO}_2$ thin films with different doping ratios.

The SiO_2 -doped TiO_2 films demonstrate significant potential for applications across various fields. In photocatalysis, the increased surface area and decreased electron-hole pair recombination improve the efficiency of degradation of organic contaminants by photocatalysis. In solar cells, the increased optical band gap renders these films suitable for applications requiring UV absorption, contributing to improved performance. Furthermore, in environmental remediation, the amorphous $\text{TiO}_2\text{:SiO}_2$ films, with their enhanced surface properties, are effective in the treatment of wastewater and air pollutants.

4. Solar cell characteristics

The samples were investigated for use as an active layer in dye-sensitized solar cells (DSSCs). Pure TiO_2 and TiO_2 supplemented with various ratios of SiO_2 were tested, and the results showed that the solar cell based on $\text{TiO}_2\text{:SiO}_2$ at a ratio of 1:0.1 improved the performance by 23 times compared to the solar cell based on TiO_2 alone. The increase is due to the improvement in Estimating the density of short-circuit current (J_{sc}) from 2.73 to 7.51 mA/cm^2 , which is due to the improved charge transport due to the improved surface structure of the films as shown in the AFM and SEM images, which enhances the absorption properties and current density. The improvement in J_{sc} resulted in the power conversion efficiency (PCE) rising from 0.07% to 2.57%, and the fill factor (FF) increased from 17% to 62% due to the improvement in the series resistance (R_s) and branch resistance (R_{sh}). With the increase of SiO_2 to 0.3, the J_{sc} increased to 11.71 mA/cm^2 , but the increase of SiO_2 led to a decrease in R_{sh} , which negatively affected the cell performance such as FF and PCE, while the high concentration of SiO_2 led to a deterioration in the performance of solar cells Table 3 shows the solar cell parameters based on different SiO_2 enriched TiO_2 ratio.

Table 3. Solar cell parameters based on different SiO_2 ratio doped TiO_2 .

SiO_2 Ratio	J_{sc} ($\text{mA} \cdot \text{cm}^{-2}$)	V_{oc} (Volt)	F F %	PCE %	R_s ($\text{k}\Omega$)	R_{sh} ($\text{M}\Omega$)
0	2.73	0.152	17	0.07	33.33	30.303
0.1	7.51	0.552	62	2.58	1.7	289.636
0.2	11.71	0.52	34	2.07	1.7	27.3
0.3	7.57	0.5	30	1.15	2	39.66
0.4	6.66	0.5	30	1.01	2.5	37.74

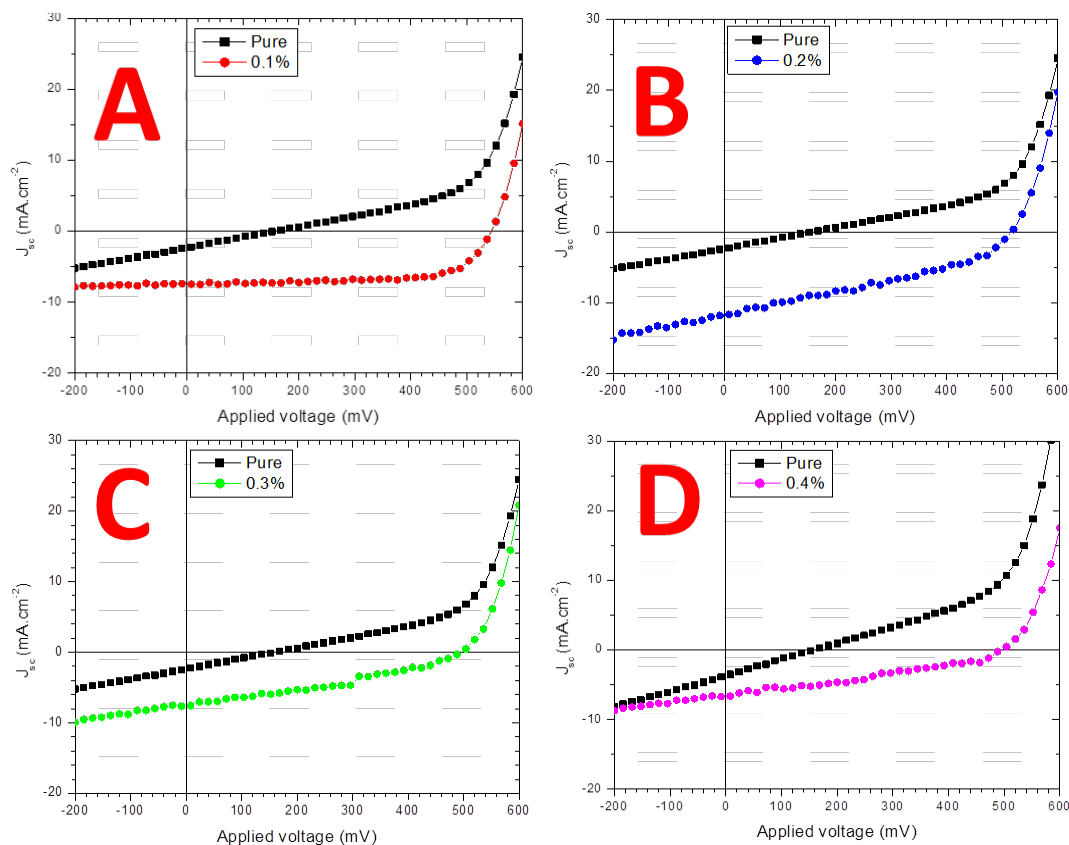


Fig. 9. Solar cell characteristics with different SiO_2 ratios.

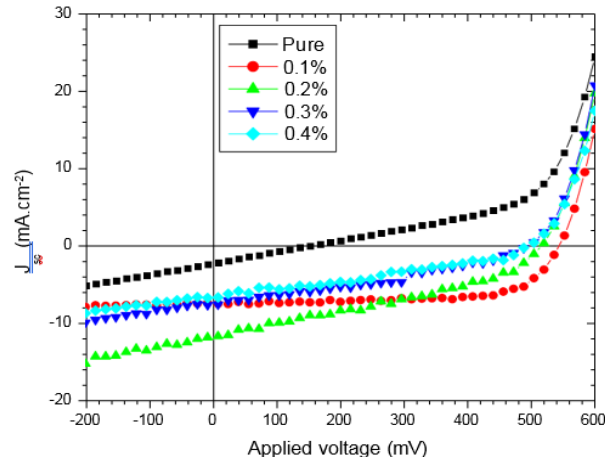


Fig. 10. Shows all the solar cell parameters for the $\text{TiO}_2\text{:SiO}_2$ samples under study with different trend.

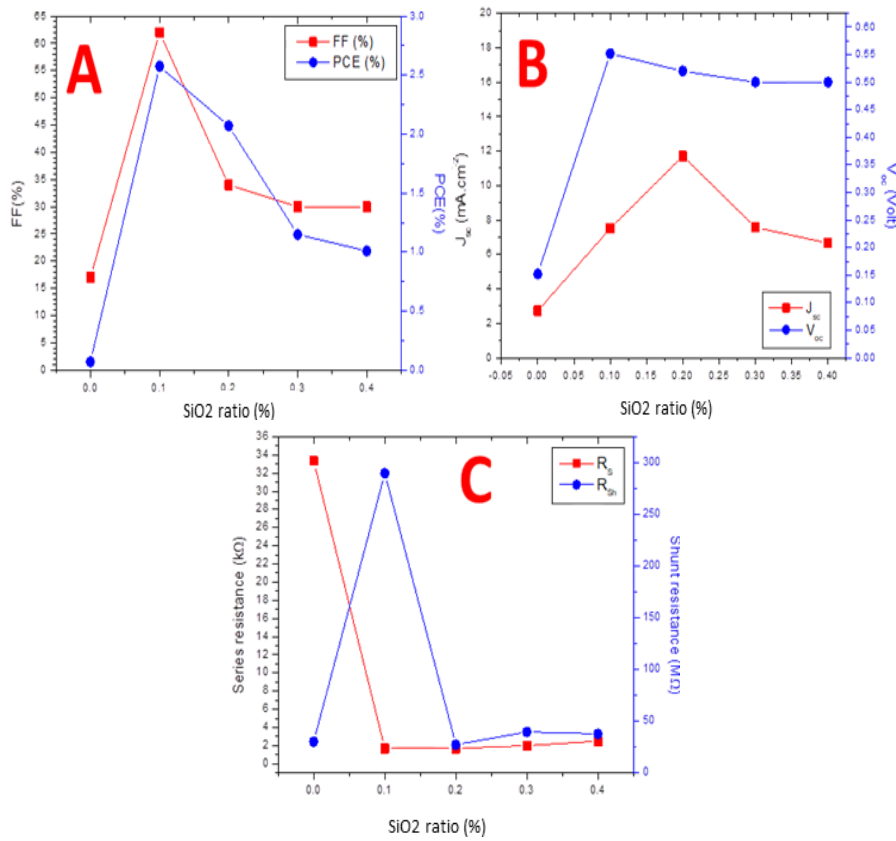


Fig. 11. Solar cell parameters with different ratios of SiO_2 , A: FF and PCE, B: J_{sc} and V_{oc} , C: R_s and R_{sh} .

5. Conclusion

In this research, the consequence of SiO_2 addition on the structural, optical, and surface properties of TiO_2 thin films prepared using the gel-solidification method was studied. The results showed that SiO_2 significantly affects the crystalline structure of TiO_2 , causing a gradual transformation from crystalline to amorphous phases with increasing SiO_2 ratio. It was found that when adding silica at ratios of (0.1), which are considered somewhat low, the anatase phase remained dominant, while on the other hand, when using ratios of 0.3 and 0.4, we found that there was a significant decrease in the crystalline phase, which is considered useful in some applications.

X-ray diffraction (XRD) showed that there is a shift from the crystalline phase when adding silica to (TiO₂), where we notice the shift of some peaks as the obtained data shows. It also showed that there is a clear increase in the crystal sizes as the concentration of silica added to titanium increases.

On the other hand, AFM and scanning electron microscope (SEM) analysis showed that adding silica will definitely affect the surface roughness, as the roughness features increase as the doping percentage increases. As for the optical properties, the results of the UV examination showed that the doping process caused an increase in the energy gap, which is considered useful in photocatalytic processes. When the doping process occurred and the nanoparticles were formed, which led to an increase in the surface to volume ratio, in addition to reducing the electron-gap formation processes in the produced films, all of which led to improving the light transmission properties and catalytic efficiency, as the results of TiO₂:SiO₂ films in solar cells showed better performance than the elements that include TiO₂ only, especially in the sample that had a low doping ratio compared to the higher ratios. Where the results of the solar cells deteriorated at these ratios.

In the end, the most important conclusion we can draw from this research is that the doping processes that are low will certainly lead to an increase in the efficiency of the solar cell, according to the efficiency factor that was calculated.

References

- [1] Das, S., Lenka, T. R., Talukdar, F. A., Velpula, R. T., Nguyen, H. P. T. (2023), Optical and Quantum Electronics, 55(1), 67; <https://doi.org/10.1007/s11082-022-04350-y>
- [2] Jawad, M. H., & Abdulameer, M. R. (2023), Iraqi Journal of Science, 1210-1218; <https://doi.org/10.24996/ij.s.2023.64.3.17>
- [3] Li, Y., Zha, C., Yan, X., Yuan, X., Zhang, Y., Zhang, J., Zhang, X. (2024), Optical and Quantum Electronics, 56(3), 378; <https://doi.org/10.1007/s11082-023-05893-4>
- [4] A. J. Frank, N. Kopidakis, J. Van De Lagemaat, Coord. Chem. Rev., vol. 248, no. 13-14, pp. 1165-1179, (2004); <https://doi.org/10.1016/j.ccr.2004.03.015>
- [5] Fahem MQ, Hassan TA., Karbala International Journal of Modern Science. 2022;8(4):651-6; <https://doi.org/10.33640/2405-609X.3265>
- [6] W. M. Campbell, A. K. Burrell, D. L. Officer, K. W. Jolley, Coord. Chem. Rev., vol. 248, no. 13-14, pp. 1363-1379, (2004); <https://doi.org/10.1016/j.ccr.2004.01.007>
- [7] R. Xie, C. R. López-Barrón, N. J. Wagner, ACS Publications, pp. 83-142. (2017); <https://doi.org/10.1021/bk-2017-1250.ch005>
- [8] R. Daghrir, P. Drogui, D. Robert, Ind. Eng. Chem. Res., vol. 52, no. 10, pp. 3581-3599, (2013); <https://doi.org/10.1021/ie303468t>
- [9] M. H. Jawad, A. A. Assi, A. M. Hameed, Plasmonics; <https://doi.org/10.1007/s11468-025-02828-5>
- [10] M. Q. Fahem, T. A. A. Hassan, Iraqi J. Sci., pp. 4740-4748, (2022); <https://doi.org/10.24996/ij.s.2022.63.11.13>
- [11] R. K. Jamal, F. H. Ali, M. M. Hameed, K. A. Aadim, Iraqi J. Sci., pp. 1032-1039, (2020); <https://doi.org/10.24996/ij.s.2020.61.5.12>
- [12] Salman, O. N., Ismail, M. M., Dawood, M. O. (2023), Optical and Quantum Electronics, 55(5), 469; <https://doi.org/10.1007/s11082-023-04741-9>
- [13] K. Pournemati, A. Habibi-Yangjeh, A. Khataee, Inorg. Chem., vol. 63, no. 15, pp. 6957-6971, (2024); <https://doi.org/10.1021/acs.inorgchem.4c00440>
- [14] A. K. Mohsin, S. D. Madhloom, K. A. Aadim, AIP Conference Proceedings, AIP Publishing, (2022); <https://doi.org/10.1063/5.0096682>
- [15] M. Rasheed, M. N. Mohammedali, F. A. Sadiq, M. A. Sarhan, T. Saidani, J. Opt., pp. 1-15, (2024); <https://doi.org/10.1007/s12596-024-01928-5>
- [16] S. W. Glunz, F. Feldmann, Sol. Energy Mater. Sol. Cells, vol. 185, pp. 260-269, (2018); <https://doi.org/10.1016/j.solmat.2018.04.029>

- [17] Din, M. U., Mumtaz, M., Qasim, I. (2024), Optical and Quantum Electronics, 56(10), 1622; <https://doi.org/10.1007/s11082-024-07491-4>
- [18] M. H. Jawad, M. R. Abdulameer, AIP Conference Proceedings, AIP Publishing, 2024; <https://doi.org/10.1063/5.0183126>
- [19] S. Maurya et al., J. Opt., pp. 1-6, (2025); <https://doi.org/10.1007/s12596-025-02450-y>
- [20] S. H. M. Salleh, M. Z. M. Yusoff, Sci. Res. J., vol. 20, no. 1, pp. 1-11, (2023); <https://doi.org/10.24191/srj.v20i1.19056>
- [21] S. Sahoo et al., J. Opt., pp. 1-16, 2024; <https://doi.org/10.1007/s12596-024-02255-5>
- [22] M. A. F. Md Fauzi, M. H. Razali, M. U. Osman, B. Mohd Azam, Adv. Mater. Process. Technol., vol. 8, no. 4, pp. 4395-4415, (2022); <https://doi.org/10.1080/2374068X.2022.2076976>
- [23] Rashid, T. M., Rahmah, M. I., Mahmood, W. K., Fahem, M. Q., Jabir, M. S., Bidan, A. K., Alsaffar, S. M. (2025), Plasmonics, 1-12; <https://doi.org/10.1007/s11468-025-02874-z>